Supplementary Information

Natural biomass-based multifunctional conductive composite films integrating personal thermal management, electromagnetic interference shielding, physiological signal sensing

Songyu Han, Xugang Dang*, Jiajia Tang, Xuechuan Wang

Institute of Biomass and Function Materials & National Demonstration Centre for Experimental Light Chemistry Engineering Education, College of Bioresources Chemistry and Materials Engineering, Shaanxi University of Science and Technology, Xi'an, 710021, PR China

*Corresponding author: xg.dang@sust.edu.cn (X Dang)

Number of Pages: 18

Number of Figure: 5 (Fig. S1-Fig. S5)

Number of Tables: 7 (Table S1-Table S7)

DCS preparation

According to the previous study, 20 g of CS and 29.3 g of NaIO4 were dissolved in 270 mL of deionized water, and the reaction was carried out at 35 ℃ for 48 h under the protection of light. Subsequently, the sample was washed with anhydrous ethanol and deionized water alternately for 4~5 times until the DCS was free of impurities. The washed sample was then transferred to a vacuum drying oven and dried at 40 ℃ for 24 h to obtain DCS white powder (yield: 88%). The oxidation degree of DCS was determined using the hydroxylamine hydrochloride method, and the oxidation degree was calculated to be 62.8% according to Equations 1-1, 1-2, and 1-3.

Characterisation of DSA and DSAC

FTIR

The DSA and DSAC were tested using an FTIR spectrometer (Vertex70, Bruker, Germany) at room temperature with a resolution of 4 cm^{-1} in the range of 400 to 4000 cm^{-1} .

XRD

Changes in the crystalline behaviour of DSA and DSAC were tested by means of a wide angle X-ray diffractometer (XRD, D8 Advance Bruker, Germany) with Cu-K radiation. The scanning angle 2θ ranged from 5° to 60° .

XPS

The elemental composition of the samples was analysed using an X-ray photoelectron spectrometer (KRATOS, Ultra DLD, UK) for DSAC. In this, the vacuum of the analysis chamber was 9.8×10^{-10} Torr and the excitation source was Al ka-rays (hv= 1486.6 eV). The full-spectrum acquisition voltage was 15 kV, the filament current was 5 mA, and the test flux energy Pass Energy was 160 eV; the fine-spectrum voltage was 15 kV, the filament current was 10 mA, and the test flux energy Pass Energy was 40 eV. Charge correction was performed using the C1s= 284.80 eV binding energy

as the energy standard.

Thermal analysis

The thermal stability of the DSA and DSAC was tested using a thermogravimetric analyser (TA Instrument Q500) and a differential scanning calorimeter (TA Instruments DSC Q2000).The DSA and DSAC were subjected to TGA in a nitrogen atmosphere at a heating rate of 10 ℃/min-1 over a temperature range of 40 ℃ to 600 ℃.

Surface morphology

The surface and cross-sectional morphology of the DSA and DSAC were observed by scanning electron microscopy (SEM) with the test voltage set at 7 kV, and the bacterial morphology on the test films was observed using a high-resolution field emission scanning electron microscope (FEI Verios 460, FEI, U.S.A.) with the test voltage set at 2 kV, and the physical morphology on the surfaces of the DSA and DSAC were observed by a three-dimensional super-depth-of-field microscope (HIROX, Japan). and DSAC film surfaces were observed through a three-dimensional ultra-deep field microscope (HIROX (HOSCOPE), Japan).

Transmittance and colour value evaluation

The DSA and DSAC were cut into 3 mm × 3 mm squares, and the light transmittance of the DSA and DSAC samples was evaluated by a UV-visible-NIR spectrophotometer (Cary 5000, Agilent, USA) in the wavelength range of 200-800 nm, with air as a control.

The colour parameters of the DSA and DSAC were measured using a colour matching system (Ci7800, Axiom X-Rite, USA), where L* denotes luminance, a* denotes red/green and b* denotes yellow/blue. The measurement was repeated three times for each sample to take the average value, and the total colour difference (Δ E*) of DSA and DSAC were calculated according to equation (1).

$$\Delta E^{*}=\sqrt{(L^{*}-L_{s}^{*})^{2}+(a^{*}-a_{s}^{*})^{2}+(b^{*}-b_{s}^{*})^{2}} \qquad (1)$$

where , and are the colour parameters of the standard whiteboard (= 93.58, = 1.54 and = -0.50) and L*, a* and b* are the colour parameters of the DSA and DSAC film samples.

Water contact angle

The hydrophilicity of DSA and DSAC were characterised by the magnitude of the water contact angle (WCA) on a video optical contact angle meter (OCR20, Germany). A drop of distilled water (5 μL) was deposited on the film surface with a precision syringe, and after 3 s, the contact angle on both sides of the droplet was measured using the OSA100 software and the average value was calculated. The measurements were repeated five times for each set of samples to take the average value.

Water vapour permeability

The water vapour transmission coefficient (WVP) of DSA and DSAC were determined using a water vapour transmission rate tester (Jinan Labthink Electro-mechanical Technology Co., Ltd.), and the measurements were repeated three times for each sample to take the average value. The parameters of the tester were set to maintain the temperature at 38 ° C and the relative humidity at 90 %.

Mechanical and adhesion properties

The stress-strain curves were obtained by cutting the DSA and DSAC into dumbbell shapes of 2 mm × 35 mm and measuring them using an electronic universal testing machine (Yangzhou Xintianhui Electronic Technology Co., Ltd., China). The measurements were repeated six times for each group of samples to take the average value.

Firstly, market-bought pig skins were soaked in PBS buffer at room temperature in order to remove the remaining fat adhering to the surface. Subsequently, the pigskin was cut into thin slices of approximately 3 cm × 1 cm and immersed in PBS again. Before use, the residual liquid on the surface of the pork skin was gently blotted with

filter paper. The (1 cm × 1 cm × 2 mm) film was adhered between two pieces of pigskin and pressed continuously for 1 min. then, the prepared samples were left at room temperature for 3 h. Finally, the adhesive properties were tested by performing lap shear test on a material testing system at a speed of 5 mm-min^{-1} . Then, the adhesion of substrates such as wood panels was tested according to the above method. And its adhesion performance on the surface of plastic, rubber, paper, leather, glass, metal and other materials was analysed. The DSAC film was also placed on human joints to test its adhesion ability to human skin.

Antimicrobial properties of DSA and DSAC

Bacterial culture

The microorganisms Escherichia coli (E. coli) and Staphylococcus aureus (S. aureus) were used to evaluate the antimicrobial properties of DSA and DSAC. All bacterial strains were passaged at 37 ° C for 24 h on LB agar medium.

Circle of inhibition test

The antimicrobial activity of DSA and DSAC were evaluated using the disc diffusion method, and the experimental results were expressed as the mean diameter of the inhibitory circle in millimetres ± standard deviation (mean ± standard deviation). The brief procedure was as follows: the test samples (6 mm in diameter), which had been sterilised by UV for 5 min, were laid flat in a medium coated with 100 μL of bacterial suspension, after which the medium was incubated in a thermostatic incubator at 37° C for 24 h. All experiments were carried out in triplicate.

Minimum Inhibitory Concentration (MIC) Coated Plate Assay

The strains were inserted into the liquid medium and incubated overnight at 37° C in a constant temperature incubator. With a pipette gun, 1 mL of the strain was loaded into a test tube containing 9 mL of sterile saline (also available culture medium)

and mixed thoroughly, this is the 10^{-1} dilution, and so on to make 10^{-2}、10^{-3}、10^{-4}、10^{-5}、10^{-6} and 10^{-7} several dilutions of the strain, and measure the OD600 values of different concentrations. Take 200 μL of 10^{-4}, 10^{-5} and 10^{-6} concentration bacterial solution for coating experiment, three groups in parallel for each gradient, adjust the concentration of bacterial suspension, and determine the concentration of its bacterial solution by plate colony counting method, so that the number of bacteria it contains is 1~2×108 CFU/mL, that is, it is the bacterial suspension for the donor.The DSA and DSAC are cut into small discs with a diameter of 6 mm, and sterilised under ultraviolet light for 5 min before the test. The DSA and DSAC were immersed in 10 mL of bacterial solution and incubated for 24 h. After 24 h, the DSA and DSAC were placed in 10 mL of sterile saline, sonicated for 5 min, and then 20 μL of the films were coated with beef paste peptone agar medium and incubated at 37 ℃ for 24 h. The UV-sterilised filter paper with a diameter of 6 mm was used as the control group. All experiments were performed in triplicate.

Antioxidant activity

DPPH

The DPPH method of Xia was referenced and slightly modified for the determination of antioxidant activity of DSA and DSAC. Firstly, 3.9 mg of DPPH was accurately weighed and dissolved in 50 mL of ethanol to prepare the DPPH free radical. Small film discs of 4 × 6 mm were placed into 3.6 mL of the free radical solution, mixed well, and kept in a test tube for a certain period of time to ensure adequate reaction. Finally, the UV absorbance at 517 nm was recorded to calculate the DPPH radical scavenging rate according to equation (2).

$$\text{DPPH inhibition (\%)} = \frac{A_0 - A_i}{A_0} \times 100 \quad (2)$$

Where A_0 is the absorbance of pure DPPH solution at 517 nm; A_i is the

absorbance of DPPH solution treated with DSA and DSAC at 517 nm.

ABTS

Twenty mg of ABTS was mixed with 5 mL of 2.4 mol/L potassium persulfate solution and reacted for 12 h away from light to form $ABTS^+$ radical. Dilute the stock solution to 100 mL with anhydrous ethanol so that the absorbance at 734 nm (OD value) was 0.70 ± 0.02. Take different mass concentrations of the sample solution (e.g., 100 μL) and add them to 1.9 mL of the ABTS working solution, shake well, and then react for 6 min under the protection of light. Repeat the above steps with anhydrous ethanol instead of the sample solution and determine the absorbance (noted as A1); the absorbance of the sample group (Ai) and the blank control group (A1) was measured at 734 nm, and the ABTS radical scavenging rate was calculated by the following formula (3)

$$\text{ABTS inhibition (\%)} = \frac{A_0 - Ai + A_1}{A_0} \times 100 \quad (3)$$

Where, A_0: absorbance of anhydrous ethanol instead of sample (control); A_i: absorbance of sample group (A1); A_1: absorbance of anhydrous ethanol instead of ABTS solution.

Biocompatibility Test

Cytotoxicity of DSA and DSAC were assessed by CCK-8 assay using hamster lung cells (CHL). Firstly, a 96-well plate was inoculated with 100 μL of cell suspension (1×105 cells mL-1) and incubated in 5% CO_2, 37° C atmosphere for 24 h to allow the cells to adhere to the wall. Afterwards, the original medium was poured out, and the wells with 200 μL of RPMI1640 complete medium were used as the control group, and the wells with 200 μL of DSA and DSAC film extracts were used as the experimental group. 20 μL of CCK-8 (at a concentration of 5 mg mL-1) was added to each well on days 1, 3, and 5 of the cell culture, and the incubation was continued for 2 h at 5 % CO_2 and 37 ° C. The absorbance of each well was

measured at 450 nm. The absorbance of each well was measured at 450 nm. The absorbance values of each group were entered into Excel and the relative viability was calculated (relative viability % = (OD value of the experimental group)/(mean OD value of the control group) × 100%); dead/living cells were assessed by staining with the Calcein-AM/PI Cell Double Staining Kit, and living cells were indicated by green fluorescence, while dead cells were indicated by red fluorescence.

Photothermal conversion test

The photothermal properties of the DSAC film were evaluated using a NIR laser with a wavelength of 980 nm. The DSAC film was cut into small discs of 2 cm diameter and the DSAC film was irradiated using NIR light, then a thermometer was used to record the temperature values at the time point and around the irradiation point of the film, and the data was recorded as the temperature was further stabilised. The same method was used to test the photothermal performance of the laser at different powers. For the cyclic photothermal test of DSAC film, NIR light was first irradiated on the surface of DSAC film, and when the surface temperature of DSAC film reached the peak, the NIR light was removed and the surface temperature of DSAC film was left to drop to room temperature. Throughout the process, a thermometer was used to record the DSAC film surface temperature, and the process was repeated three times.

Electromagnetic Shielding Test

The electromagnetic shielding performance of the thin films was tested by the coaxial method, i.e. in the range of 8.2 GHz to 12.4 GHz, using a vector network analyser (VNA) and a coaxial test fixture. Calculation of total shielding effectiveness (SET) and reflection/absorption attenuation by measuring the scattering parameters of the sample.

Flexible Sensing Tests

Thin films were made into flexible strain sensors and resistance was measured in real time on a two-electrode test cell at an electrochemical workstation. The strain sensitivity (GF) was calculated according to equation (4) below:

$$GF = \frac{\Delta R/R_0}{\varepsilon} \quad (4)$$

Where: R_0 is the initial resistance of the film in Ω;

ΔR is the change resistance in Ω;

ε is the applied strain.

The sensors were subsequently applied to monitor human joint movements, subtle facial expression changes, physiological signals, speech, etc., aiming to explore the potential applications of DSAC in the fields of health monitoring, emotion detection and human-computer interaction.

Secondly, the hydrogel temperature sensor was tested as follows: water in a beaker was heated to a constant temperature by a heating station, and then the hydrogel sensor, which was connected to the electrochemical workstation and sealed with a medical PU film, was immersed in the constant temperature water. When the resistance signal in the electrochemical workstation is stable, the resistance value is recorded and the TCR value is calculated.

The TCR value is calculated according to the following formula (5):

$$TCR = \frac{Rt - R_0}{R_{0^{\Delta T}}} \quad (5)$$

Where: Rt is the instantaneous resistance at the measurement temperature;

R0 is the instantaneous resistance at the reference temperature;

Δ T is the temperature difference.

The test method of the ‘Skin Contact Temperature Warning Device’ is as follows: the water in the beaker is heated to a constant temperature by a heating

table, and then the hydrogel sensor connected to the electrochemical workstation is contacted with the surface of the beaker at different temperatures for 5 s. At the same time, the change in resistance is recorded by the electrochemical workstation and the change in temperature is recorded by the infrared thermal imaging camera.

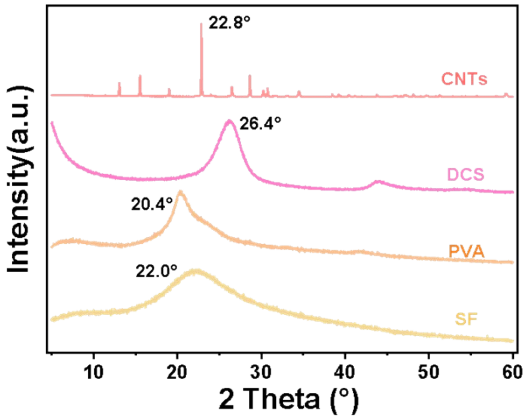

Fig. S1 XRD diffraction patterns of the raw materials

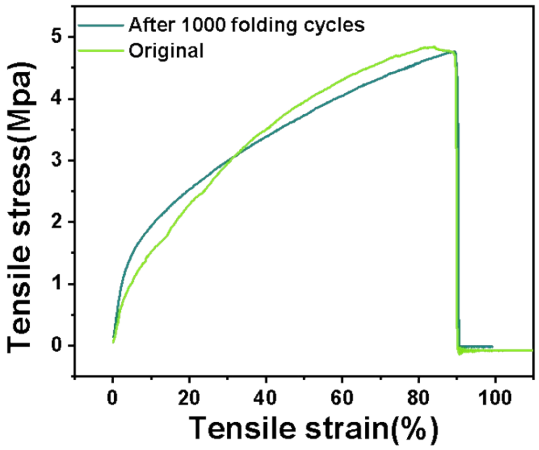

Fig. S2 Stretch performance of DSAC after 1000-fold folding

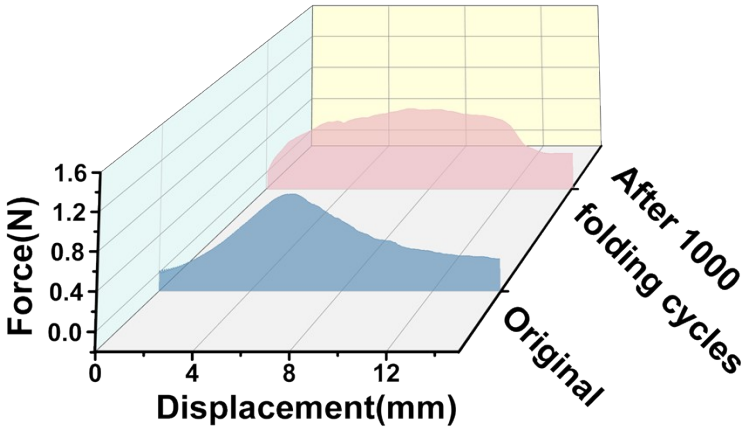

Fig. S3 Adhesion performance of DSAC on pig skin after 1,000-fold folding

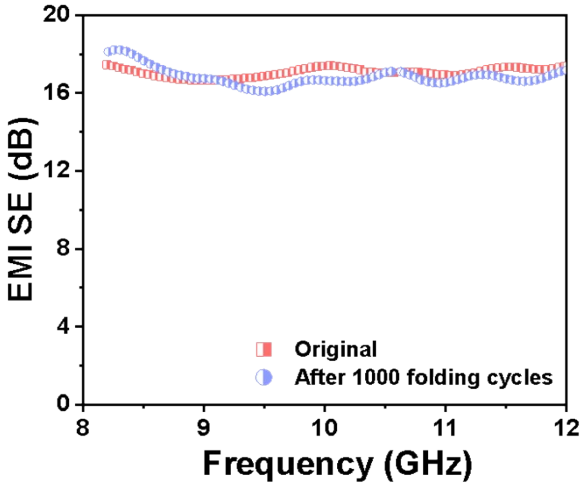

Fig. S4 EMI SE of DSACafter 1,000-fold Folding at 8.2-12.4 GHz frequency

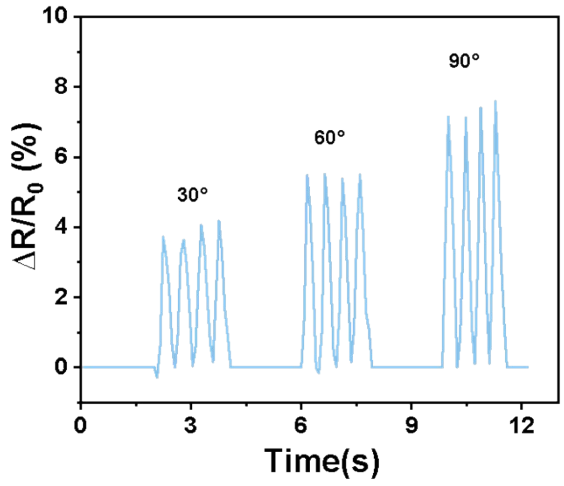

Fig. S5 Relative resistance variation of DSAC at different finger flexion angles after

three months of ambient storage

Table S1 T_{max1}, T_{max2}, T_{max3} of DSA and DSAC

	DSA	DSAC1	DSAC2	DSAC3	DSAC4
T_{max1}/℃	121.39	108.31	107.33	120.66	125.14
T_{max2}/℃	240.42	250.73	249.80	255.83	253.43
T_{max3}/℃	460.34	458.37	458.45	457.70	449.00
T50/℃	344.14	322.22	332.78	327.25	348.78
CY/%	33.8	30.3	32.7	30.44	32.67

Table S2 L*, a*, b* and ΔE* colour parameters and transmittance characteristics of DSA and DSAC

Films	L*	a*	b*	ΔE*	T_{280}(%)	T_{660}(%)
DSA	79.81±0.62	-1.83±0.42	44.00±0.92	46.70	2.370	83.750
DSAC1	54.4±4.50	14.07±2.49	24.89±2.65	48.33	0.030	65.190
DSAC2	47.75±0.23	8.54±0.61	12.91±0.73	48.26	0.020	38.81
DSAC3	36.15±0.34	1.67±0.29	8.63±0.53	58.15	0.010	26.280
DSAC4	44.61±0.98	0.26±1.07	6.65±0.99	49.50	0.010	12.59

Table S3 Adhesion mechanism analysis of DSAC on metal substrate

Component	Active group	Mechanism of action
DCS	$-COO^-$	Forms chelate bonds with metal oxides (e.g. Fe_2O_3/Al_2O_3)
AgNPs	Ag^+	Penetrates into metal microcracks, forms metal-silver bonds and covalently binds to metal atoms.
SF	$-NH_3^+$	Adsorption of negatively charged metal oxides by electrostatic attraction.
PVA	-OH	Hydrogen bonding via water molecule bridging
CNTs	-COOH	Hydrogen bonding with metal oxides

Table S4 Adhesion mechanism analysis of DSAC on paper substrate

Component	Active group	Mechanism of action
DCS	-OH， -CHO	-OH forms a hydrogen bond with cellulose -OH; -CHO forms a hemiacetal bond with cellulose terminal -OH: R-CHO + HO-cellulose → R-CH(OH)-O-cellulose
PVA	-OH	Penetration of paper fibre pores and formation of hydrogen bonding network (dominant role)
SF	-CONH-	Hydrogen bonding with cellulose-OH
AgNPs	Ag^{+}	Coordination with reducing groups (e.g. aldehyde groups) in cellulose, inhibiting microbial degradation
CNTs	nano-roughness structure	Physically embedded in fibre pores

Table S5 Adhesion mechanism analysis of DSAC on leather substrate (collagen/lipid complex)

Component	Active group	Mechanism of action
SF	Hydrophobic structural domain (β-folding region)	Binding of leather oils and fats by hydrophobic action
AgNPs	Ag^{+}	Forms ligand bonds with collagen cysteines
DCS	-COOH	Forms hydrogen bonds with collagen peptide bonds
PVA	$-CH_2-$	Hydrophobic linkage between methylene and lipid chains
CNTs	Cutting-edge nanostructures	Mechanical puncture of leather collagen microfibres

Table S6 Composition and dosage of raw materials

Samples	DCS/g	SF/g	PVA/g	Glycerol/g	AgNPs/g	CNTs/g	H_2O/mL
DSA	1	2	0.9	0.39	0	0	80
DSAC1	1	2	0.9	0.39	0.0043	0.0043	80
DSAC2	1	2	0.9	0.39	0.0043	0.0107	80
DSAC3	1	2	0.9	0.39	0.0043	0.0215	80
DSAC4	1	2	0.9	0.39	0.0043	0.0429	80

Table S7 Comparison of Electromagnetic Shielding Performance between DSAC and Biomass-Based Composites

Samples	Name	Thickness/mm	EMI SE/dB	Ref
1	graphite/starch coating（One-side coating）	0.03	2.5	[1]
2		0.06	5	
3		0.09	9.5	
4		0.12	11.5	
5		0.3	16.5	
6	graphite/starch coating（Two-side coating）	0.03	7.8	
7		0.06	12	
8		0.09	15.5	
9	PPF/TCT	0.3762	24.3	[2]
10	NFAG-600	2.5	1	[3]
11	NFAG-700	2.5	12	
12	rL1C20	0.155	20.5	[4]
13	rL3C20	0.155	21.5	

14	NCF1:9	0.25	3.5	[5]
15	NCF3:7	0.25	15.5	
16	1-0-1	1	5	[6]
17	1-1-1	1	24	
18	WA	2.5	19	[7]
19	AgNWs@CS-PDMS-2	2	14	[8]
20	d-AgNWs@CS-PDMS-2	2	19	
This work	DSAC	0.2	18	

Reference

[1] Y. Yang, J.-R. Tao, D. Yang, Q.-M. He, X.-D. Chen, M. Wang, Improving dispersion and delamination of graphite in biodegradable starch materials via constructing cation-π interaction: towards microwave shielding enhancement, Journal of Materials Science & Technology 129 (2022) 196-205.

[2] J. Wei, P. Zhao, D. Li, P. Xie, S. Wang, C. Tang, G. Fei, L. Dai, Sandwich structured cellulose-based composite for electromagnetic interference shielding, infrared stealth and Joule heating, Carbohydrate Polymers (2025) 123979.

[3] P. Chen, S. He, T. Wang, C. Wang, J. Tao, Y. Li, Melanin-like nanofibers with highly ordered structures achieve ultrahigh specific electromagnetic interference shielding efficiency, Nature Communications 16(1) (2025) 7127.

[4] L. Wang, D. Xu, J. Zhou, Multilayer composite films with enhanced electromagnetic interference shielding and thermal management properties based on bamboo cellulose nanofibers, Carbohydrate Polymers 354 (2025) 123309.

[5] J. Ren, C. Huang, R. Tan, J. Chen, M. Huang, M. Wang, W. Liu, B. Li, Z. Ma, L. Wang, All-Biomass Nanocomposite Films via Facile and Sustainable Design Procedure for Thermal Management and Electromagnetic Interference Shielding, Advanced Science 12(43) (2025) e10372.

[6] M. Cheng, M. Ying, R. Zhao, L. Ji, H. Li, X. Liu, J. Zhang, Y. Li, X. Dong, X. Zhang, Transparent and flexible electromagnetic interference shielding materials by constructing sandwich AgNW@ MXene/wood composites, ACS nano 16(10) (2022) 16996-17007.

[7] J. Chen, Z. Zhu, H. Zhang, S. Tian, S. Fu, Wood-derived nanostructured hybrid for efficient flame retarding and electromagnetic shielding, Materials & Design 204 (2021) 109695.

[8] M. Zhu, X. Yan, Y. Lei, J. Guo, Y. Xu, H. Xu, L. Dai, L. Kong, An ultrastrong and antibacterial silver nanowire/aligned cellulose scaffold composite film for

electromagnetic interference shielding, ACS Applied Materials & Interfaces 14(12) (2022) 14520-14531.